INORGANIC CHEMISTRY
FRONTIERS

RESEARCH ARTICLE

View Article Online
View Journal | View Issue

Cite this: *Inorg. Chem. Front.*, 2023, **10**, 621

Construction of a π-stacked supramolecular framework using a triphenylene-cored metallo-organic cage†

Zhilong Jiang,‡[a] Jun Wang,‡[a] Mingzhao Chen,*[a] Chaolong Tang,[c] He Zhao,[b] Qiangqiang Dong,[b] Wei-Dong Yu,[b] Zhiyuan Jiang,[b] Bangtang Chen,[a] Xiaorui Li,[b] Die Liu,[b] Liao-Yuan Yao,[d] Hui Liu,[b] Ting-Zheng Xie,[a] Tun Wu,[a] Jie Yuan,[e] Kun Wang,[c] Yiming Li*[b] and Pingshan Wang*[a,b]

Supramolecular nanocages with inner cavities have attracted increasing attention due to their fascinating molecular aesthetics and vast number of potential applications. Even though a wide array of discrete supramolecular cages with precisely designed sizes and shapes have been established, the controlled assembly of higher-order supramolecular frameworks from discrete molecular entities still represents a formidable challenge. In this work, a novel metallo-organic cage **[$Zn_{12}L_4$]** was assembled based on a triphenylene-cored hexapod terpyridine ligand. Synchotron X-ray analysis revealed a pair of enantiomeric cages in the crystal with flexible ligands twisted clockwise or anticlockwise due to steric hindrance in the structure. Interestingly, due to the strong π–π intermolecular interaction between triphenylene units, a controlled hierarchical packing of sphere-like cages in the crystal was established having a sparse packing mode with huge channels of around 3.6 nm diameter. This research sheds light on the design of strong π–π interactions in supramolecular hierarchical packing and materials science.

Received 3rd October 2022,
Accepted 23rd November 2022

DOI: 10.1039/d2qi02125k

rsc.li/frontiers-inorganic

Introduction

Molecular nanocages with a well-defined inner space have shown advanced applications in the fields of molecular recognition,[1–6] catalysis,[7–10] separation,[11–14] and so on. In the past few decades, numerous three-dimensional (3D) nanocages of various sizes and shapes were created using different synthetic approaches, such as hydrogen bonding,[15,16] metal–organic coordination,[17–20] dynamic covalent chemistry[21,22] and so on. Among these nano-structures, metal–organic cages based on coordination-driven self-assembly have received a lot of attention from scientists in the past three decades due to the highly predictable nature of coordination bonds and the precise designability of the organic ligand.[23–28] Benefiting from their well-designed inner cavities, such metallo-cages have found useful applications in chemical sensing,[29–31] catalysis,[32–35] drug delivery[36–38] and host–guest chemistry.[39–42] Because of these advanced functional applications, chemists are paying much attention to the construction of supramolecular cages with unique three-dimensional structures.

Hierarchical superstructures that are comprised of discrete molecular entities are expected to yield solubility-enhanced molecular porous materials that are different from metal–organic frameworks (MOFs).[43] Even though a wide array of discrete supramolecular cages with precisely designed sizes and shapes have been established, the controlled assembly of higher-order supramolecular frameworks from discrete molecular entities still represents a formidable challenge. Approaches to assemble cages into porous frameworks through supramolecular interactions in order to achieve better application performances are still unusual. Weak noncovalent interactions (such as metal coordination, multiple hydrogen

[a]*Institute of Environmental Research at Greater Bay Area; Guangzhou Key Laboratory for Clean Energy and Materials; Key Laboratory for Water Quality and Conservation of the Pearl River Delta, Ministry of Education, Guangzhou University, Guangzhou, 510006 Guangdong, China. E-mail: jinyulinzhao@foxmail.com, chemwps@csu.edu.cn*
[b]*College of Chemistry and Chemical Engineering; School of Metallurgy and Environment, Central South University, Changsha, 410083 Hunan, China. E-mail: chemyl@csu.edu.cn*
[c]*Department of Physics Astronomy; Department of Chemistry, Mississippi State University, Mississippi, MS 39762, USA*
[d]*MOE Key Laboratory of Cluster Science; School of Chemistry and Chemical Engineering, Beijing Institute of Technology, Beijing, 102488 Beijing, China*
[e]*School of Chemistry and Chemical Engineering, Henan Normal University, Xinxiang, 453007 Henan, China*

†Electronic supplementary information (ESI) available: Synthetic procedures, NMR spectra, ESI-MS spectra and SCXRD data, and supporting figures and table. CCDC 2109206. For ESI and crystallographic data in CIF or other electronic format see DOI: https://doi.org/10.1039/d2qi02125k

‡These authors contributed equally to this work.

bonding, host–guest interactions and aromatic stacking) have been employed as major driving forces in intermolecular chemistry.[44–46] The π-stacking interaction is even more important in controlling the orientation of a hierarchical assembly into higher-order architectures.

In this work, we report the self-assembly of a pair of enantiomeric metallo-organic cages by employing a C_{3v} symmetric hexapod ligand. In order to control the higher-order superstructural packing of the cage, triphenylene, one of the larger aromatic molecules with extensive π-systems, was introduced into the ligand as the core. Tridentate terpyridine (tpy) motifs were used as the connection units towards metals due to their extraordinary coordination ability and stability with most transition metal ions and their achievements in constructing numerous supramolecular architectures.[47–49] After coordinating with Zn^{2+} ions, the hexapod building blocks lose their σ_v mirror symmetry during the formation of the supramolecule, and a twisted truncated tetrahedral cage $[\mathbf{Zn_{12}L_4}]$ is obtained. The single crystal X-ray diffraction of $[\mathbf{Zn_{12}L_4}]$ revealed that due to the steric hindrance between adjacent coordination junctions in the cage, the flexible ligands twist clockwise or anticlockwise and generate a pair of enantiomers $[\mathbf{Zn_{12}L_4}]^{-A}$ and $[\mathbf{Zn_{12}L_4}]^{-C}$ (Scheme 1). By controlling the π–π stacking between triphenylene units, the hierarchical packing of the supramolecular cages reveals large triple helix channels of 3.6 nm diameter, which can be classified as 3(1,1,2) using the nomenclature of parastichy. The introduction of such fused-ring molecules to induce supramolecular cage stacking is of great significance for the construction of porous-frame structures, as well as in host–guest chemistry, resolution and other fields.

Results and discussion

Self-assembly and characterization of metallo-organic cages

A C_{3v} symmetric hexapod ligand **L** was synthesized through a 6-fold Suzuki coupling reaction on 2,3,6,7,10,11-hexabromotriphenylene. The supramolecular cage was formed by treating ligand **L** with 3 equivalents of $Zn(NO_3)_2{\cdot}6H_2O$ in $CHCl_3$/MeOH. After precipitating with an excess amount of NH_4PF_6, the metallo-organic cage $[\mathbf{Zn_{12}L_4}]$ was obtained as a pale yellow solid in nearly quantitative yield.

NMR spectroscopy was first used to confirm the synthesis of supramolecular cage $[\mathbf{Zn_{12}L_4}]$. From the ^{1}H NMR spectrum of ligand **L** in Fig. 1A, only one set of characteristic tpy-unit peaks was observed, indicating the same chemical environment of all six tpy arms and the high symmetry of the ligand. Interestingly, after the coordination, two sets of tpy-unit signals appeared in the aromatic region of $[\mathbf{Zn_{12}L_4}]$ (Fig. 1B). This result suggested that by forming the cage structure, the symmetry of the ligand was decreased due to the limit of arm rotation and the twist of the ligand, leading to a difference of tpy chemical environments and splitting of the signals. All of the signal peaks were fully assigned under the assistance of homonuclear chemical shift correlation spectroscopy (COSY) and nuclear Overhauser effect spectroscopy (NOESY). Compared with the ^{1}H NMR spectrum of **L**, the characteristic peaks of tpy-$H^{6,6''}$ in the supramolecule were shifted and split from 8.59 to 7.60 and 7.49 ppm due to electron shielding effects, indicating the coordination of terpyridine units with Zn^{2+} ions. Very uncommonly, the singlet of tpy-$H^{3',5'}$ protons at 8.53 ppm was split into two singlets at 9.33 (down-field shift) and 8.07 ppm (up-field shift) with an integration ratio of 1 : 1. From the NOESY spectrum, spatial correlations were observed between the two adjacent terpyridine arms on the same benzene ring, such as A-H^c with B-H^b and B-H^c, and A-tpy-$H^{3',5'}$ with B-tpy-$H^{3,3''}$, respectively (Fig. S8†). Such correlations explained the unusual chemical shift caused by electron shielding effects of spatially adjacent aromatic rings in the condensed structure.[50,51] In addition, the signals substantiated that these two sets of signal peaks belonged to one supramolecular structure.

Moreover, diffusion-ordered spectroscopy (DOSY) was used to further confirm the component singleness of the assembled

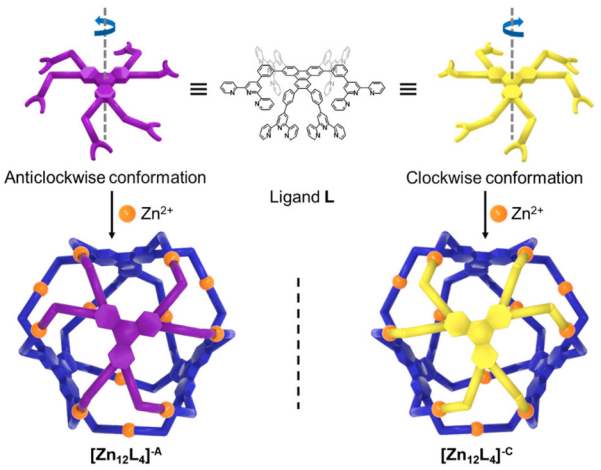

Scheme 1 Self-assembly of enantiomeric chiral metallo-organic cages $[\mathbf{Zn_{12}L_4}]^{-A}$ and $[\mathbf{Zn_{12}L_4}]^{-C}$.

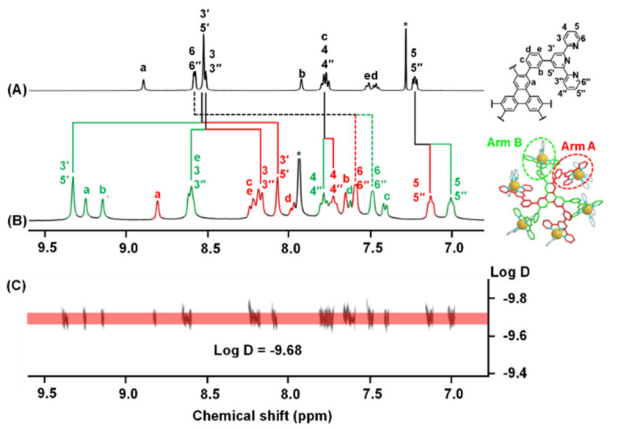

Fig. 1 (A) The ^{1}H NMR spectrum of ligand **L** in $CDCl_3$. (B) The ^{1}H NMR spectrum of $[\mathbf{Zn_{12}L_4}]$ in DMF/CD_3CN. (C) The 2D DOSY spectrum of $[\mathbf{Zn_{12}L_4}]$ in DMF/CD_3CN.

product. In Fig. 1C, the spectrum exhibited a narrow band at $\log D = -9.68$ corresponding to the ^{1}H NMR spectrum (Fig. 1B), further indicating only one supramolecular component in the self-assembly process. Based on the Stokes–Einstein equation, the hydrodynamic radius (r_H) was calculated as 1.4 nm (as shown in Fig. S11†), which also agreed well with the radius measured in the single-crystal structure.

To further investigate the composition of the assembled product, the supramolecule was tested by electrospray ionization mass spectrometry (ESI-MS) and traveling wave ion mobility mass spectrometry (TWIM-MS) experiments. The ESI-MS spectrum of $[\mathbf{Zn_{12}L_4}]$ revealed a series of peaks at m/z = 996.00, 1110.11, 1249.31, 1424.11, 1648.09, 1946.76, and 2364.90 corresponding to the continuous charge states from 11+ to 5+ due to the successive loss of PF_6^- counterions (Fig. 2A). After deconvolution, the molecular weight of the metallo-organic cage $[\mathbf{Zn_{12}L_4}]$ was calculated as 12 529 Da, which revealed a composition of $[\mathbf{Zn_{12}L_4}]^{24+}$ with 24 PF_6^- anions. In addition, the experimental isotopic patterns of all charge states agreed well with the corresponding theoretically calculated values of $[\mathbf{Zn_{12}L_4}]$ (the results can be found in Fig. S14†). Furthermore, the TWIM-MS plot of $[\mathbf{Zn_{12}L_4}]$ showed a narrow drift time at charge states from 11+ to 7+, further indicating the absence of other supramolecular structures (Fig. 2B).

On account of the strong affinity between triphenylene and fullerenes through π–π stacking, C60 was selected to investigate the host–guest chemistry of the supramolecular cage. The encapsulation of a fullerene occurs upon mixing C60 simultaneously with the metallo-organic cage $[\mathbf{Zn_{12}L_4}]$ in DMF/CH_3CN, followed by heating at 90 °C for 24 h. The ESI-MS spectrum revealed a series of continuous signal peaks of host–guest molecule C60⊂$[\mathbf{Zn_{12}L_4}]$, indicating the successful encapsulation of the guest molecule C60 in the supramolecular cage $[\mathbf{Zn_{12}L_4}]$ (Fig. S20†).

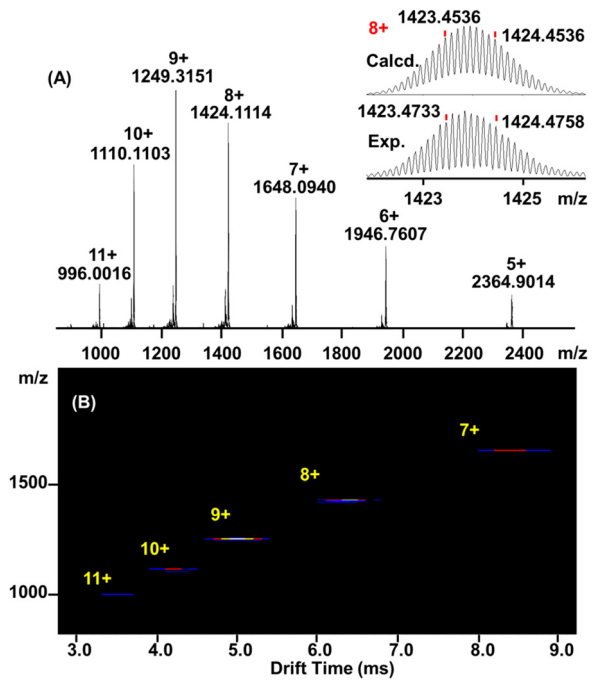

Fig. 2 (A) The ESI-MS spectrum of $[\mathbf{Zn_{12}L_4}]$. (B) A TWIM-MS plot of $[\mathbf{Zn_{12}L_4}]$.

Crystal structure of $[\mathbf{Zn_{12}L_4}]$

To unambiguously reveal the structure of the assembled supramolecule, single crystal X-ray diffraction was performed using a synchrotron source. However, it is extremely difficult to grow single crystals of suitable quality in 3D nanocages based on terpyridine self-assembly. Hitherto, only four crystal structures of terpyridine-based nanocages have been reported.[52–55] Fortunately, a crystal of $[\mathbf{Zn_{12}L_4}]$ was achieved through slow evaporation of ethyl acetate into a solution of $[\mathbf{Zn_{12}L_4}]$ in DMF at a constant temperature of 298 K (Fig. S22†). Crystal structure analysis revealed that the $[\mathbf{Zn_{12}L_4}]$ supramolecule adopts a truncated tetrahedron-like shape with a decreased T_d symmetry, composed of four triangular faces and six ship-like dimeric faces. The triangular faces were formed by the connection of terpyridines at the *ortho*-position of the same benzene, while the ship-like dimeric faces were formed by the connection of terpyridines to spaced benzene rings. Interestingly, in the same unit cell, a pair of enantiomeric cages were discovered with the hexapod ligand twisted clockwise (named as $[\mathbf{Zn_{12}L_4}]^{-C}$) or anticlockwise (named as $[\mathbf{Zn_{12}L_4}]^{-A}$) (Fig. 3A). It is worth noting that the chirality of the structures arose on account of symmetry breaking caused by the configuration differences of the ligand. The ideal truncated tetrahedron belongs to T_d point group symmetry with one C_3 symmetric axis and three mirror planes across the center of the triangular face. However, in such an ideal structure, the ship-like dimeric faces would have to overcome a large steric hindrance between the two swollen ⟨tpy-Zn^{2+}-tpy⟩ junctions. Thus, to sustain a cage structure with less steric hindrance, these two adjacent ⟨tpy-Zn^{2+}-tpy⟩ units adopt staggered positions that cause the twisting of the ligand, leading to a loss of mirror planes and the formation of two heterochiral enantiomers. Many attempts have been tried in order to isolate these enantiomeric structures. However, unlike chiral organic cages, which can be isolated by chiral HPLC, their separation was not successful probably due to the reversibility of the coordination bonds and the high polarity of the metallo-cages.

3D packing analysis of the $[\mathbf{Zn_{12}L_4}]$ cage

In many spherical cage systems, hierarchical packing in the crystal is usually compact as the closest packing system for a sphere (face-centred cubic) has no large interspaces. In the crystal of $[\mathbf{Zn_{12}L_4}]$, strong intermolecular π–π stacking interactions between triphenylene planes at the truncated vertices of the cage were observed, with two triphenylenes at a distance of 3.5 Å being interlaced at a 60° angle (Fig. 3B). Interestingly, in benefiting from the π–π intermolecular interaction, such a sphere-like cage formed a sparse packing mode with huge channels of around 3.6 nm diameter (Fig. 4A). With such columnar cavities, this type of superstructural framework may have potential applications in the fields of electronics,[56,57] catalysis,[58,59] energy storage,[60,61] separation[62–64] and so

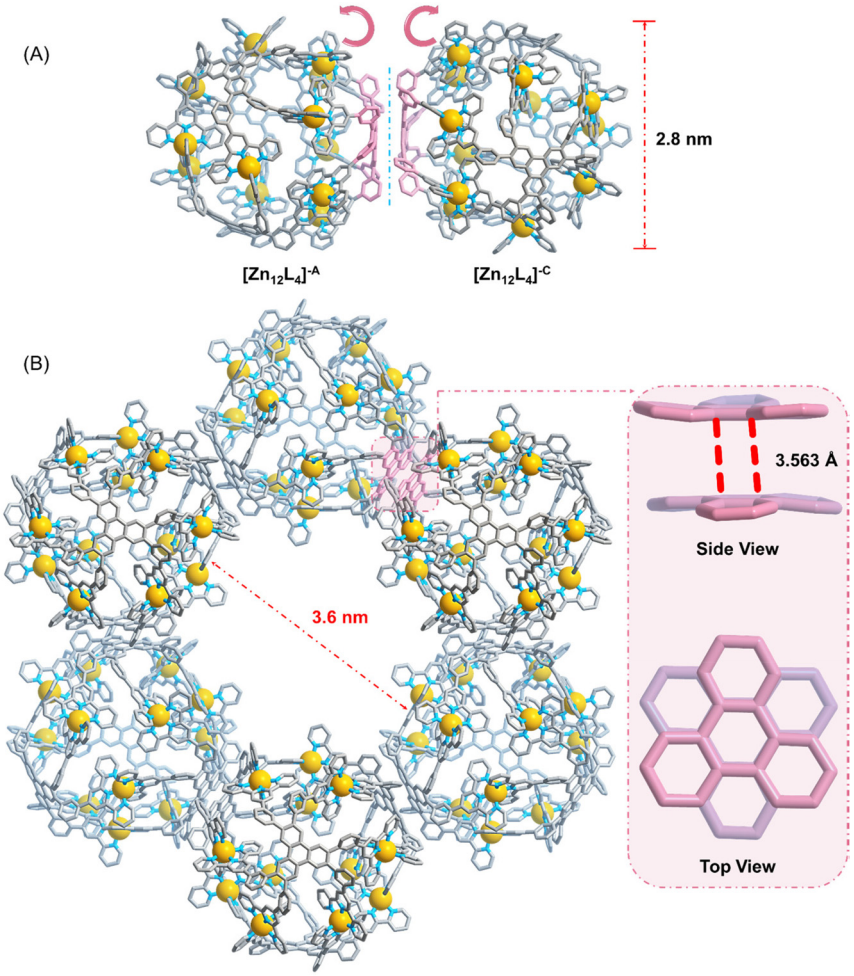

Fig. 3 (A) Crystal structure of enantiomeric supramolecular cages $[Zn_{12}L_4]^{-A}$ and $[Zn_{12}L_4]^{-C}$. (B) A π-stacked supramolecular framework based on the π–π intermolecular interaction between triphenylene units.

on.[65,66] Through careful observation, we found that the prominent tpy coordination junctions around the channels are not mirror symmetric, but instead exhibited anti-clockwise or clockwise patterns (Fig. S25†) from different viewpoints. To illustrate the detailed structure, the tpy units vertical to the channel are colored red, while the tpy units parallel to the channel are colored blue (Fig. 4B). From the top view, red tpy can be regarded as an arrowhead and blue tpy as an arrow shaft. By extrapolating the cages upwards along the arrow direction, three helices are seen to be present in each superstructural channel (Fig. 4C), forming an intertwined complementary triple helix structure, which is similar to the collagen structure in biological systems.[67,68]

Furthermore, the triple helix packing of the $[Zn_{12}L_4]$ metallo-organic cage can be classified as 3(1,1,2) according to the nomenclature of natural parastichy, which is the spiral arrangement of leaves or scales in biological systems.[69,70] By simplifying the helical elements using isotropic spheres, the parastichy pattern of 3(1,1,2) is as shown in Fig. 5A. To illustrate the helical arrangement while retaining the symmetry of the pattern, the column can be unrolled along the screw axis onto a plane. In this plane, all of the spheres can be connected in series with three red dashed lines, indicating the features of a triple helix structure (Fig. 5B). By unrolling the superstructural channel in the crystal of $[Zn_{12}L_4]$, the metallo-organic cage exhibits exactly the same pattern as the packing of parastichy 3(1,1,2) and reveals its natural parastichy structure.

For the cage enantiomers, the hierarchical packing revealed that the two enantiomeric cages coexist in the crystal structure with a 1 : 1 ratio, and align alternately into a "Kagome" topology pattern (Fig. S27B†).[71,72] In the same layer, each truncated tetrahedral cage is in contact with three other upside-down enantiomeric cages through their triangular faces. From the side view in Fig. S27C,† enantiomers $[Zn_{12}L_4]^{-C}$ and $[Zn_{12}L_4]^{-A}$ are arrayed in separate straight lines with the different enantiomers in opposite directions. In these packing lines, each truncated tetrahedron makes contact with an upper or lower one *via* contact of triangular faces with hexagonal faces. As shown in Fig. S26E,† one of the four triphenylene planes in the cage has no π–π stacking with any other and simply faces the hollow

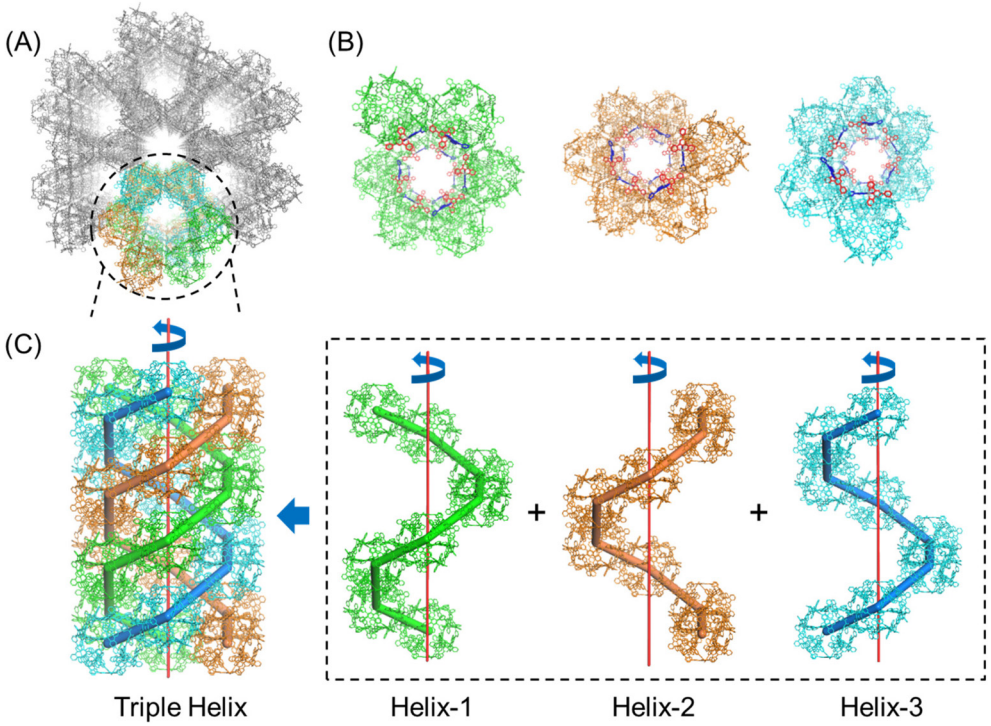

Fig. 4 (A) 3D packing analysis of metallo-organic cages. (B) Top view of three helices in perspective projection. (C) A triple helix structure formed by the intertwining of three complementary helices.

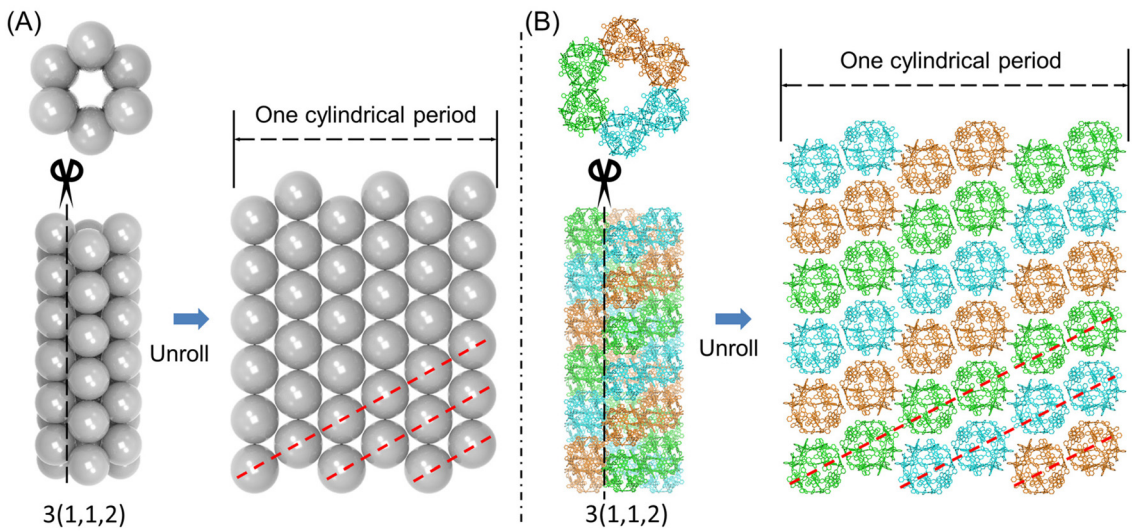

Fig. 5 A comparison of the helical arrangement of sphere models and that of the metallo-organic cage $[Zn_{12}L_4]$. (A) Helical arrangement of isotropic spheres with parastichy pattern 3(1,1,2), which can be unrolled along the columnar axis into the topological plane on the right. (B) Helical packing of metallo-organic cages around channels in the crystal structure.

center of the coordination triangle formed by the neighboring cage in the same packing line.

AFM and STM of the $[Zn_{12}L_4]$ cage

To obtain more detailed information about the $[Zn_{12}L_4]$ metallo-organic cage, atomic force microscopy (AFM) and scanning tunneling microscopy (STM) were applied to visualize the supramolecules directly. In STM, a linear packing structure was observed on the surface of highly oriented pyrolytic graphite (HOPG). We speculated that such a superstructure is attributed to π–π interactions between the triphenylene of supramolecule $[Zn_{12}L_4]$ and the HOPG surface, as well as the π–π stack-

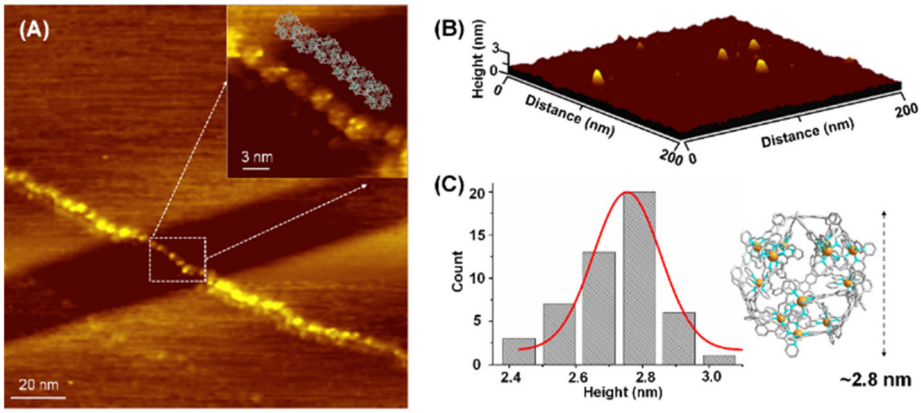

Fig. 6 STM and AFM of metallo-organic cage $[Zn_{12}L_4]$. (A) STM images of a fiber-like nanostructure on a HOPG surface. (B) An AFM image of the metallo-organic cage $[Zn_{12}L_4]$. (C) A statistical histogram of the AFM image for 50 particles.

ing and van der Waals' interaction between cages (Fig. 6A). The AFM images were obtained by dropping a diluted DMF solution of $[Zn_{12}L_4]$ (4×10^{-5} M) onto a freshly cleaved mica surface. In Fig. 6B, discrete particles were clearly observed with similar diameters and, in total, 50 dots were counted with the size distribution as shown in Fig. 6C. These results showed that most of the particles possessed a height of around 2.8 nm, which perfectly matches the size of the target supramolecular cage.

Conclusions

In summary, we have synthesized a pair of enantiomeric metallo-organic cages by employing an achiral hexapod ligand with high C_{3v} symmetry. The single crystal X-ray diffraction analysis revealed that due to the steric hindrance between adjacent ⟨tpy-Zn^{2+}-tpy⟩ connections, all of the faces in the structure twist either clockwise or anticlockwise and generate a pair of enantiomers $[Zn_{12}L_4]^{-C}$ and $[Zn_{12}L_4]^{-A}$. Benefiting from the strong π–π intermolecular interaction between triphenylene units, the hierarchical packing of sphere-like cages in the crystal was controlled to give a sparse packing mode with huge channels of around 3.6 nm diameter, where such channels revealed triple helix structures that conformed exactly to the same pattern as that of natural parastichy 3(1,1,2). This research not only allows for the use of steric hindrance to construct chiral supramolecular cages, but also sheds light on the design of strong π–π interactions in supramolecular hierarchical packing and materials science.

Author contributions

Z.J. and P.W. designed the experiments. Z.J. and J.W. completed the synthesis. B.C., H.Z. and Q.D. analyzed the NMR experimental data; M.C. and Z.J. performed the MS characterization. T.X., T.W. and W.L. contributed to X-ray data collection; L.Y. and W.Y. contributed to crystallographic analysis. C. T. and K.W. contributed to AFM and STM analyses; Z.J., J.W., M.C. and Y.L. analyzed the data and wrote the manuscript. P. W., M.C., D.L., H.L. and X.L. revised and supervised the writing of the manuscript. All the authors discussed the results and commented on, and proofread the manuscript.

Conflicts of interest

There are no conflicts to declare.

Acknowledgements

We acknowledge support from the National Natural Science Foundation of China (21971257, 22101060, 22101302) the Hunan Provincial Science and Technology Plan Project of China (No. 2019TP1001), the Excellent Youth Funding of Hunan Provincial Science and Technology Department (2022JJ20053), and the Science and Technology Research Project of Guangzhou (202201020201; 202102010432). K. Wang acknowledges support from the U.S. National Science Foundation (OIA-1757220). We thank staff from the BL17B beamline of the National Facility for Protein Science Shanghai (NFPS) at the Shanghai Synchrotron Radiation Facility for their assistance during data collection.

References

1 M. Yamashina, Y. Tanaka, R. Lavendomme, T. K. Ronson, M. Pittelkow and J. R. Nitschke, An antiaromatic-walled nanospace, *Nature*, 2019, **574**, 511–515.
2 S. Hasegawa and G. H. Clever, Metallo-supramolecular Shell Enables Regioselective Multi-functionalization of Fullerenes, *Chem*, 2020, **6**, 5–7.
3 Y. Wang, Y. Zhang, Z. Zhou, R. T. Vanderlinden, B. Li, B. Song, X. Li, L. Cui, J. Li, X. Jia, J. Fang, C. Li and

P. J. Stang, A cyclic bis[2]catenane metallacage, *Nat. Commun.*, 2020, **11**, 2727.

4 H. Duan, Y. Li, Q. Li, P. Wang, X. Liu, L. Cheng, Y. Yu and L. Cao, Host–Guest Recognition and Fluorescence of a Tetraphenylethene-Based Octacationic Cage, *Angew. Chem., Int. Ed.*, 2020, **59**, 10101–10110.

5 H. Takezawa, R. Tabuchi, H. Sunohara and M. Fujita, Confinement of Water-Soluble Cationic Substrates in a Cationic Molecular Cage by Capping the Portals with Tripodal Anions, *J. Am. Chem. Soc.*, 2020, **142**, 17919–17922.

6 Y. Chen, G. Wu, B. Chen, H. Qu, T. Jiao, Y. Li, C. Ge, C. Zhang, L. Liang, X. Zeng, X. Cao, Q. Wang and H. Li, Self-Assembly of a Purely Covalent Cage with Homochirality by Imine Formation in Water, *Angew. Chem., Int. Ed.*, 2021, **60**, 18815–18820.

7 Z. Zhou, J. Liu, J. Huang, T. W. Rees, Y. Wang, H. Wang, X. Li, H. Chao and P. J. Stang, A self-assembled Ru-Pt metallacage as a lysosome-targeting photosensitizer for 2-photon photodynamic therapy, *Proc. Natl. Acad. Sci. U. S. A.*, 2019, **116**, 20296–20302.

8 W. Cullen, H. Takezawa and M. Fujita, Demethylenation of Cyclopropanes via Photoinduced Guest-to-Host Electron Transfer in an M_6L_4 Cage, *Angew. Chem., Int. Ed.*, 2019, **58**, 9171–9173.

9 T. A. Bender, R. G. Bergman, K. N. Raymond and F. D. Toste, A Supramolecular Strategy for Selective Catalytic Hydrogenation Independent of Remote Chain Length, *J. Am. Chem. Soc.*, 2019, **141**, 11806–11810.

10 K. Omoto, S. Tashiro and M. Shionoya, Phase-Dependent Reactivity and Host–Guest Behaviors of a Metallo-Macrocycle in Liquid and Solid-State Photosensitized Oxygenation Reactions, *J. Am. Chem. Soc.*, 2021, **143**, 5406–5412.

11 L. Ma, C. J. E. Haynes, A. B. Grommet, A. Walczak, C. C. Parkins, C. M. Doherty, L. Longley, A. Tron, A. R. Stefankiewicz, T. D. Bennett and J. R. Nitschke, Coordination cages as permanently porous ionic liquids, *Nat. Chem.*, 2020, **12**, 270–275.

12 H. Zeng, M. Xie, T. Wang, R.-J. Wei, X.-J. Xie, Y. Zhao, W. Lu and D. Li, Orthogonal-array dynamic molecular sieving of propylene/propane mixtures, *Nature*, 2021, **595**, 542–548.

13 P. C. Purba, M. Maity, S. Bhattacharyya and P. S. Mukherjee, A Self-Assembled Palladium(II) Barrel for Binding of Fullerenes and Photosensitization Ability of the Fullerene-Encapsulated Barrel, *Angew. Chem., Int. Ed.*, 2021, **60**, 14109–14116.

14 C.-X. Chen, Z.-W. Wei, T. Pham, P. C. Lan, L. Zhang, K. A. Forrest, S. Chen, A. M. Al-Enizi, A. Nafady, C.-Y. Su and S. Ma, Nanospace Engineering of Metal–Organic Frameworks through Dynamic Spacer Installation of Multifunctionalities for Efficient Separation of Ethane from Ethane/Ethylene Mixtures, *Angew. Chem., Int. Ed.*, 2021, **60**, 9680–9685.

15 L. Adriaenssens and P. Ballester, Hydrogen bonded supramolecular capsules with functionalized interiors: the controlled orientation of included guests, *Chem. Soc. Rev.*, 2013, **42**, 3261–3277.

16 D. Ajami, L. Liu and J. Rebek Jr., Soft templates in encapsulation complexes, *Chem. Soc. Rev.*, 2015, **44**, 490–499.

17 T. R. Cook, Y.-R. Zheng and P. J. Stang, Metal–Organic Frameworks and Self-Assembled Supramolecular Coordination Complexes: Comparing and Contrasting the Design, Synthesis, and Functionality of Metal–Organic Materials, *Chem. Rev.*, 2013, **113**, 734–777.

18 D. Zhang, T. K. Ronson and J. R. Nitschke, Functional Capsules via Subcomponent Self-Assembly, *Acc. Chem. Res.*, 2018, **51**, 2423–2436.

19 Y. Sun, C. Chen, J. Liu and P. J. Stang, Recent developments in the construction and applications of platinum-based metallacycles and metallacages via coordination, *Chem. Soc. Rev.*, 2020, **49**, 3889–3919.

20 E. G. Percástegui, T. K. Ronson and J. R. Nitschke, Design and Applications of Water-Soluble Coordination Cages, *Chem. Rev.*, 2020, **120**, 13480–13544.

21 M. Mastalerz, Porous Shape-Persistent Organic Cage Compounds of Different Size, Geometry, and Function, *Acc. Chem. Res.*, 2018, **51**, 2411–2422.

22 K. Acharyya and P. S. Mukherjee, Organic Imine Cages: Molecular Marriage and Applications, *Angew. Chem., Int. Ed.*, 2019, **58**, 8640–8653.

23 C. M. Hong, R. G. Bergman, K. N. Raymond and F. D. Toste, Self-Assembled Tetrahedral Hosts as Supramolecular Catalysts, *Acc. Chem. Res.*, 2018, **51**, 2447–2455.

24 C. T. McTernan, J. A. Davies and J. R. Nitschke, Beyond Platonic: How to Build Metal-Organic Polyhedra Capable of Binding Low-Symmetry, Information-Rich Molecular Cargoes, *Chem. Rev.*, 2022, **122**, 10393–10437.

25 J. Zhao, Z. Zhou, G. Li, P. J. Stang and X. Yan, Light-emitting self-assembled metallacages, *Natl. Sci. Rev.*, 2021, **8**, nwab045.

26 E. Sánchez-González, M. Y. Tsang, J. Troyano, G. A. Craig and S. Furukawa, Assembling metal-organic cages as porous materials, *Chem. Soc. Rev.*, 2022, **51**, 4876–4889.

27 Y. Domoto and M. Fujita, Self-assembly of nanostructures with high complexity based on metal unsaturated-bond coordination, *Coord. Chem. Rev.*, 2022, **466**, 214605.

28 M. Chen, J. Wang, D. Liu, Z. Jiang, Q. Liu, T. Wu, H. Liu, W. Yu, J. Yan and P. Wang, Highly Stable Spherical Metallo-Capsule from a Branched Hexapodal Terpyridine and Its Self-Assembled Berry-type Nanostructure, *J. Am. Chem. Soc.*, 2018, **140**, 2555–2561.

29 X. Yan, T. R. Cook, P. Wang, F. Huang and P. J. Stang, Highly emissive platinum(II) metallacages, *Nat. Chem.*, 2015, **7**, 342–348.

30 M. Han, R. Michel, B. He, Y.-S. Chen, D. Stalke, M. John and G. H. Clever, Light-Triggered Guest Uptake and Release by a Photochromic Coordination Cage, *Angew. Chem., Int. Ed.*, 2013, **52**, 1319–1323.

31 P. Mal, B. Breiner, K. Rissanen and J. R. Nitschke, White phosphorus is air-stable within a self-assembled tetrahedral capsule, *Science*, 2009, **324**, 1697–1699.

32 D. M. Kaphan, M. D. Levin, R. G. Bergman, K. N. Raymond and F. D. Toste, A supramolecular microenvironment strategy for transition metal catalysis, *Science*, 2015, **350**, 1235–1238.

33 P. P. Neelakandan, A. Jiménez, J. D. Thoburn and J. R. Nitschke, An Autocatalytic System of Photooxidation-Driven Substitution Reactions on a $Fe^{II}_4L_6$ Cage Framework, *Angew. Chem., Int. Ed.*, 2015, **54**, 14378–14382.

34 H. Takezawa, T. Kanda, H. Nanjo and M. Fujita, Site-Selective Functionalization of Linear Diterpenoids through U-Shaped Folding in a Confined Artificial Cavity, *J. Am. Chem. Soc.*, 2019, **141**, 5112–5115.

35 M. Morimoto, W. Cao, R. G. Bergman, K. N. Raymond and F. D. Toste, Chemoselective and Site-Selective Reductions Catalyzed by a Supramolecular Host and a Pyridine-Borane Cofactor, *J. Am. Chem. Soc.*, 2021, **143**, 2108–2114.

36 S. K. Samanta, D. Moncelet, V. Briken and L. Isaacs, Metal–Organic Polyhedron Capped with Cucurbit[8]uril Delivers Doxorubicin to Cancer Cells, *J. Am. Chem. Soc.*, 2016, **138**, 14488–14496.

37 B. Therrien, G. Süss-Fink, P. Govindaswamy, A. K. Renfrew and P. J. Dyson, The "Complex-in-a-Complex" Cations $[(Acac)_2M\subset Ru_6(P\text{-}iPrC_6H_4Me)_6(tpt)_2(dhbq)_3]^{6+}$: A Trojan Horse for Cancer Cells, *Angew. Chem., Int. Ed.*, 2008, **47**, 3773–3776.

38 Z. Ma and B. Moulton, Recent advances of discrete coordination complexes and coordination polymers in drug delivery, *Coord. Chem. Rev.*, 2011, **255**, 1623–1641.

39 N. Singh, J.-H. Jo, Y. H. Song, H. Kim, D. Kim, M. S. Lah and K.-W. Chi, Coordination-driven self-assembly of an iridium-cornered prismatic cage and encapsulation of three heteroguests in its large cavity, *Chem. Commun.*, 2015, **51**, 4492–4495.

40 S. Fujii, T. Tada, Y. Komoto, T. Osuga, T. Murase, M. Fujita and M. Kiguchi, Rectifying Electron-Transport Properties through Stacks of Aromatic Molecules Inserted into a Self-Assembled Cage, *J. Am. Chem. Soc.*, 2015, **137**, 5939–5947.

41 P.-F. Cui, X.-R. Liu, Y.-J. Lin, Z.-H. Li and G.-X. Jin, Highly Selective Separation of Benzene and Cyclohexane in a Spatially Confined Carborane Metallacage, *J. Am. Chem. Soc.*, 2022, **144**, 6558–6565.

42 Y. Wang, B. Li, J. Zhu, W. Zhang, B. Zheng, W. Zhao, J. Tang, X.-J. Yang and B. Wu, Light-Triggered High-Affinity Binding of Tetramethylammonium over Potassium Ions by [18]crown-6 in a Tetrahedral Anion Cage, *Angew. Chem., Int. Ed.*, 2022, **61**, e202201789.

43 R.-R. Liang, S.-Y. Jiang, R.-H. A. and X. Zhao, Two-dimensional covalent organic frameworks with hierarchical porosity, *Chem. Soc. Rev.*, 2020, **49**, 3920–3951.

44 D. Luo, X. P. Zhou and D. Li, Beyond molecules: mesoporous supramolecular frameworks self-assembled from coordination cages and inorganic anions, *Angew. Chem., Int. Ed.*, 2015, **54**, 6190–6195.

45 Y. Kim, J. Koo, I. C. Hwang, R. D. Mukhopadhyay, S. Hong, J. Yoo, A. A. Dar, I. Kim, D. Moon, T. J. Shin, Y. H. Ko and K. Kim, Rational Design and Construction of Hierarchical Superstructures Using Shape-Persistent Organic Cages: Porphyrin Box-Based Metallosupramolecular Assemblies, *J. Am. Chem. Soc.*, 2018, **140**, 14547–14551.

46 G. L. Li, Z. Zhuo, B. Wang, X. L. Cao, H. F. Su, W. Wang, Y. G. Huang and M. Hong, Constructing π-Stacked Supramolecular Cage Based Hierarchical Self-Assemblies via π…π Stacking and Hydrogen Bonding, *J. Am. Chem. Soc.*, 2021, **143**, 10920–10929.

47 S. Chakraborty and G. R. Newkome, Terpyridine-Based Metallosupramolecular Constructs: Tailored Monomers to Precise 2D-Motifs and 3D-Metallocages, *Chem. Soc. Rev.*, 2018, **47**, 3991–4016.

48 Z. Gao, Y. Han, Z. Gao and F. Wang, Multicomponent Assembled Systems Based on Platinum(II) Terpyridine Complexes, *Acc. Chem. Res.*, 2018, **51**, 2719–2729.

49 D. Liu, K. Li, M. Chen, T. Zhang, Z. Li, J.-F. Yin, L. He, J. Wang, P. Yin, Y.-T. Chan and P. Wang, Russian-Doll-Like Molecular Cubes, *J. Am. Chem. Soc.*, 2021, **143**, 2537–2544.

50 R. H. Mitchell, V. S. Iyer, N. Khalifa, R. Mahadevan, S. Venugopalan, S. A. Weerawarna and P. Zhou, An Experimental Estimation of Aromaticity Relative to That of Benzene. The Synthesis and NMR Properties of a Series of Highly Annelated Dimethyldihydropyrenes: Bridged Benzannulenes, *J. Am. Chem. Soc.*, 1995, **117**, 1514–1532.

51 W. H. Miles, M. J. Robinson, S. G. Lessard and D. M. Thamattoor, Through-Space Shielding Effects of Metal-Complexed Phenyl Rings, *J. Org. Chem.*, 2016, **81**, 10791–10801.

52 T. Wu, Z. Jiang, Q. Bai, Y. Li, S. Mao, H. Yu, L. Wojtas, Z. Tang, M. Chen, Z. Zhang, T.-Z. Xie, M. Wang, X. Li and P. Wang, Supramolecular triangular orthobicupola: Self-assembly of a giant Johnson solid J27, *Chem*, 2021, **7**, 2429–2441.

53 T. Z. Xie, K. Guo, Z. Guo, W. Y. Gao, L. Wojtas, G. H. Ning, M. Huang, X. Lu, J. Y. Li, S. Y. Liao, Y. S. Chen, C. N. Moorefield, M. J. Saunders, S. Z. Cheng, C. Wesdemiotis and G. R. Newkome, Precise Molecular Fission and Fusion: Quantitative Self-Assembly and Chemistry of a Metallo-Cuboctahedron, *Angew. Chem., Int. Ed.*, 2015, **54**, 9224–9229.

54 S. Chakraborty, K. J. Endres, R. Bera, L. Wojtas, C. N. Moorefield, M. J. Saunders, N. Das, C. Wesdemiotis and G. R. Newkome, Concentration dependent supramolecular interconversions of triptycene-based cubic, prismatic, and tetrahedral structures, *Dalton Trans.*, 2018, **47**, 14189–14194.

55 S. Chakraborty, W. Hong, K. J. Endres, T. Z. Xie, L. Wojtas, C. N. Moorefield, C. Wesdemiotis and G. R. Newkome, Terpyridine-Based, Flexible Tripods: From a Highly Symmetric Nanosphere to Temperature-Dependent, Irreversible, 3D Isomeric Macromolecular Nanocages, *J. Am. Chem. Soc.*, 2017, **139**, 3012–3020.

56 M. Wang, R. Dong and X. Feng, Two-dimensional conjugated metal-organic frameworks (2D c-MOFs): chemistry and function for MOFtronics, *Chem. Soc. Rev.*, 2021, **50**, 2764–2793.

57 W. Wang, W. Zhao, H. Xu, S. Liu, W. Huang and Q. Zhao, Fabrication of ultra-thin 2D covalent organic framework nanosheets and their application in functional electronic devices, *Coord. Chem. Rev.*, 2021, **429**, 213616.
58 X. Zhao, P. Pachfule and A. Thomas, Covalent organic frameworks (COFs) for electrochemical applications, *Chem. Soc. Rev.*, 2021, **50**, 6871–6913.
59 A. Dhakshinamoorthy, A. M. Asiri and H. Garcia, 2D Metal-Organic Frameworks as Multifunctional Materials in Heterogeneous Catalysis and Electro/Photocatalysis, *Adv. Mater.*, 2019, **31**, 1900617.
60 J. Li, X. Jing, Q. Li, S. Li, X. Gao, X. Feng and B. Wang, Bulk COFs and COF nanosheets for electrochemical energy storage and conversion, *Chem. Soc. Rev.*, 2020, **49**, 3565–3604.
61 X. Cai, Y. Luo, B. Liu and H.-M. Cheng, Preparation of 2D material dispersions and their applications, *Chem. Soc. Rev.*, 2018, **47**, 6224–6266.
62 C. Zhang, B.-H. Wu, M.-Q. Ma, Z. Wang and Z.-K. Xu, Ultrathin metal/covalent-organic framework membranes towards ultimate separation, *Chem. Soc. Rev.*, 2019, **48**, 3811–3841.
63 R.-B. Lin, S. Xiang, H. Xing, W. Zhou and B. Chen, Exploration of porous metal-organic frameworks for gas separation and purification, *Coord. Chem. Rev.*, 2019, **378**, 87–103.
64 D. Wu, P.-F. Zhang, G.-P. Yang, L. Hou, W.-Y. Zhang, Y.-F. Han, P. Liu and Y.-Y. Wang, Supramolecular control of MOF pore properties for the tailored guest adsorption/separation applications, *Coord. Chem. Rev.*, 2021, **434**, 213709.
65 J. Wang and S. Zhuang, Covalent organic frameworks (COFs) for environmental applications, *Coord. Chem. Rev.*, 2019, **400**, 213046.
66 Y. Li, Z. Li, C. Chi, H. Shan, L. Zheng and Z. Fang, Plasmonics of 2D Nanomaterials: Properties and Applications, *Adv. Sci.*, 2017, **4**, 1600430.
67 P. T. Speakman, Proposed Mechanism for the Biological Assembly of Collagen Triple Helix, *Nature*, 1971, **229**, 241–243.
68 D. R. Walker, S. A. H. Hulgan, C. M. Peterson, I. C. Li, K. J. Gonzalez and J. D. Hartgerink, Predicting the stability of homotrimeric and heterotrimeric collagen helices, *Nat. Chem.*, 2021, **13**, 260–269.
69 H. Wang, K. Wang, Y. Xu, W. Wang, S. Chen, M. Hart, L. Wojtas, L.-P. Zhou, L. Gan, X. Yan, Y. Li, J. Lee, X.-S. Ke, X.-Q. Wang, C.-W. Zhang, S. Zhou, T. Zhai, H.-B. Yang, M. Wang, J. He, Q.-F. Sun, B. Xu, Y. Jiao, P. J. Stang, J. L. Sessler and X. Li, Hierarchical Self-Assembly of Nanowires on the Surface by Metallo-Supramolecular Truncated Cuboctahedra, *J. Am. Chem. Soc.*, 2021, **143**, 5826–5835.
70 R. O. Erickson, Tubular Packing of Spheres in Biological Fine Structure, *Science*, 1973, **181**, 705–716.
71 R. Pawlak, X. Liu, S. Ninova, P. D'Astolfo, C. Drechsel, J.-C. Liu, R. Häner, S. Decurtins, U. Aschauer, S.-X. Liu and E. Meyer, On-Surface Synthesis of Nitrogen-Doped Kagome Graphene, *Angew. Chem., Int. Ed.*, 2021, **60**, 8370–8375.
72 Q. Hao, Z.-J. Li, B. Bai, X. Zhang, Y.-W. Zhong, L.-J. Wan and D. Wang, A Covalent Organic Framework Film for Three-State Near-Infrared Electrochromism and a Molecular Logic Gate, *Angew. Chem., Int. Ed.*, 2021, **60**, 12498–12503.